Pamukkale Univ Muh Bilim Derg, 31(8), 1456-1468, 2025
(Special Issue of the 10th Geochemistry Symposium)

Pamukkale Üniversitesi Mühendislik Bilimleri Dergisi

Pamukkale University Journal of Engineering Sciences

Petrogenesis and geochemical evolution of mafic dikes in the Kıratlı Region (Yüksekova Complex, SE Türkiye): Evidence for tholeiitic–alkaline transition during Neo-Tethyan evolution

Kıratlı Bölgesi (Yüksekova Kompleksi, GB Türkiye) mafik dayklarının petrojenezi ve jeokimyasal evrimi: Neo-Tetis evrimi sırasında toleyitik–alkali geçişine kanıtlar

Hakan Yazıcıoğlu[1], *Tijen Üner*[2*]

[1]Institute of Natural and Applied Sciences, Van Yüzüncü Yıl University, Van, Türkiye.
hakanyzc02@gmail.com
[2]Department Geological Engineering, Faculty of Engineering, Van Yüzüncü Yıl University, Van, Türkiye.
tcakici@yyu.edu.tr

Received/Geliş Tarihi: 14.09.2025 Revision/Düzeltme Tarihi: 07.11.2025 doi: 10.65206/pajes.80745
Accepted/Kabul Tarihi: 09.11.2025 Special Issue Article/Özel Sayı Makalesi

Abstract

This study presents new petrographic and geochemical data on mafic dikes intruding the Kıratlı ophiolite (İpekyolu–Van, Eastern Anatolia), a segment of the southeastern branch of the Neo-Tethys. The dikes are mainly represented by microgabbros and diabases, composed of plagioclase and pyroxene, and display alteration features such as chloritization and sericitization. Major and trace element analyses indicate basaltic compositions that can be divided into tholeiitic and alkaline groups. Tholeiitic samples show depleted rare earth element (REE) patterns, Nb depletion, and Th enrichment, consistent with a supra-subduction zone origin, whereas alkaline samples exhibit light rare earth element (LREE)-enriched signatures and within-plate affinities, reflecting low-degree partial melting and/or crustal contamination during extensional phases. Comparisons with other ophiolitic dike suites in Türkiye suggest that the Kıratlı dikes record polyphase magmatism related to both subduction and extension. These findings provide new insights into the tectono-magmatic evolution of the southeastern Anatolian Ophiolite Belt and highlight the complex interplay of mantle heterogeneity, fractional crystallization, and tectonic processes during the closure of the Neo-Tethys.

Keywords: Eastern Anatolia, Mafic dike, Neo-tethys, Tholeiitic Basalt, Alkaline basalt.

Öz

Bu çalışma, Doğu Anadolu'da (İpekyolu–Van) yer alan Kıratlı ofiyoliti içine sokulan mafik dayklara ait yeni petrografik ve jeokimyasal verileri sunmaktadır. Neo-Tetis'in güneydoğu koluna ait bir kesiti temsil eden bu dayklar, esas olarak plajiyoklas ve piroksen içeren mikrogabro ve diyabazlardan oluşmakta, ayrıca kloritlenme ve serisitlenme gibi alterasyon özellikleri sergilemektedir. Ana ve iz element analizleri, daykların bazaltik bileşimler gösterdiğini ve toleyitik ile alkalen olmak üzere iki gruba ayrıldığını ortaya koymaktadır. Toleyitik örnekler, nadir toprak elementlerinde (REE) tükenmiş desenler, niyobyum (Nb) azalması ve toryum (Th) zenginleşmesi ile karakterize olup, bunlar bir süpra-subdüksiyon zonu (SSZ) kökenine işaret etmektedir. Buna karşılık, alkalen örnekler hafif nadir toprak elementlerince (LREE) zengin desenler ve kıtasal iç plakaya (within-plate) benzer jeokimyasal özellikler sergileyerek, düşük dereceli kısmî erimeyi ve/veya gerilmeli tektonik evreler sırasında kabuksal kontaminasyonu yansıtmaktadır. Türkiye'deki diğer ofiyolitik dayk serileriyle yapılan karşılaştırmalar, Kıratlı dayklarının hem dalma-batma hem de gerilme rejimlerine bağlı çok evreli magmatizmayı kaydettiğini göstermektedir. Bu bulgular, Güneydoğu Anadolu Ofiyolit Kuşağı'nın tektono-magmatik evrimine dair yeni bilgiler sunmakta ve Neo-Tetis Okyanusu'nun kapanışı sırasında manto heterojenliği, fraksiyonel kristallenme ve tektonik süreçlerin karmaşık etkileşimini vurgulamaktadır.

Keywords: Eastern Anatolia, Mafic dike, Neo-tethys, Tholeiitic basalt, Alkaline basalt.

1 Introduction

Ophiolitic rock assemblages are complex geological units formed by the emplacement of fragments of ancient oceanic lithosphere onto continental crust, and they are widely distributed in Türkiye as a result of the closure of the Neo-Tethys Ocean [1],[2]. These rocks not only represent mid-ocean ridge basalt (MORB) settings, but also record signatures of island arc tholeiites (IAT), back-arc basin basalts (BABB), and even alkali ocean island basalts (OIB) [3],[4]. Thus, the mafic and ultramafic rocks within ophiolites reflect the multi-stage magmatic and tectonic evolution of the region.

Globally, well-preserved ophiolites such as Troodos (Cyprus), Semail (Oman), Josephine (USA), and Betts Cove (Canada) provide important records of these processes, where mafic dikes intruding ultramafic units represent different tectonic stages [4]-[6]. These dikes typically display spilitic alteration, low-grade metamorphism, and petrographic diversity, and they are derived from subduction-enriched mantle sources.

In Türkiye, ophiolites related to the closure of the Neo-Tethys are preserved within different structural slices. Studies from Pozantı–Karsantı, Kızıldağ, Guleman, Kömürhan, and İspendere ophiolites have shown that most of them developed in supra-subduction zone (SSZ) environments [7]-[9]. For example, boninitic and tholeiitic dikes in the Pozantı–Karsantı ophiolite

*Corresponding author/Yazışılan Yazar

indicate remelting of highly depleted mantle sources by subduction-related melts, whereas the tholeiitic–alkaline associations in the Kızıldağ and Guleman ophiolites reflect multi-stage magmatism and progressive changes in magma sources [10].

Within this framework, the Kıratlı region ophiolite, located to the east of Lake Van, represents an important segment of the northern branch of the Southeastern Anatolian Ophiolite Belt. It contains harzburgite and dunite intruded by mafic dikes, reflecting the imprints of multi-stage magmatism in the region. However, no detailed petrographic and geochemical study has yet been carried out on the mafic dikes of this ophiolite.

Therefore, the aims of this study are to:

a) Characterize the petrographic and geochemical features of the mafic rocks in the Kıratlı region ophiolite,

b) Determine the chemical characteristics of the mafic dikes (tholeiitic vs. alkaline), and

c) Provide new insights into the tectonomagmatic setting of the ophiolite.

The results of this study are expected to contribute not only to understanding regional geology but also to the reconstruction of magma-generation processes during the closure of the Neo-Tethys Ocean.

2 Regional geology

The Eastern Anatolia region represents a tectonic zone where suture zones meet. Within this zone, suture zones belonging to the northern and southern branches of the Neo-Tethys, as well as the Sevan-Akera, Vedi, and Zagros sutures, are tectonically brought together. The basement of Eastern Anatolia consists of Late Cretaceous or older ophiolitic units [1]. It is known that the structure of the Eastern Anatolia region is generally composed of overthrust, nearly vertical mélange, and interbedded thrust sheets. In addition to Mesozoic ophiolites, these units also include Permian-aged neritic limestones and Paleocene-Eocene flysch/molasse assemblages. These units are unconformably overlain by shallow marine units, which then gradually transition into terrestrial sediments. All these units form an accretionary prism in the region. This accretionary prism or prism system observed in Eastern Anatolia is called the "Eastern Anatolian Accretionary Complex" [1] (Figure 1).

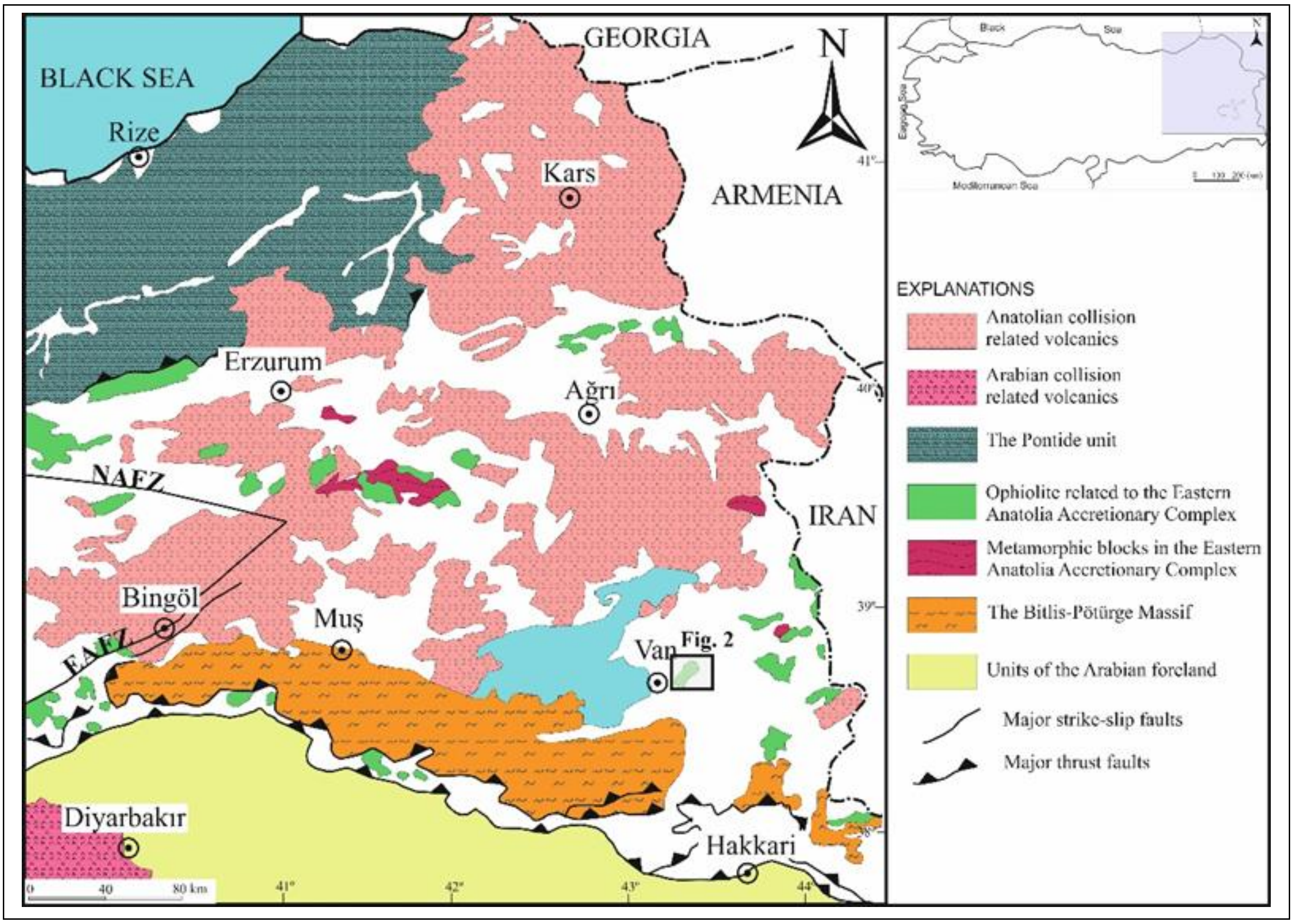

Figure 1. Simplified tectonic map of Eastern Anatolia showing the main suture zones (Sevan–Akera, Vedi, Zagros, and İzmir–Ankara–Erzincan sutures) and the location of the study area within the Eastern Anatolian Accretionary Complex [20].

The East Anatolian Accretionary Complex (EAAC), which reflects the composition of crushed-shortened continental and oceanic crustal fragments between the Arabian and Eurasian plates [11], is bounded by the Eurasian plate to the north and the Bitlis Pötürge Massif located on the northern margin of the Arabian plate to the south.

The continental collision between the Arabian and Eurasian plates began in the Middle Miocene, and the collisional processes continue today [12]-[14]. It is reported that this collision completely destroyed the Neotethyan oceanic lithosphere in Eastern Anatolia, and the EAAC assumed a dome-like shape and rose 2 km [15],[16]. The southern and eastern parts of the dike are covered by Upper Cretaceous (or younger) ophiolitic units, Upper Oligocene–Pliocene flysch deposits, and Quaternary to recent sediments. Scattered metamorphic blocks are observed with these units. These metamorphic blocks are considered fragments of the Anatolide-Tauride microcontinent [17], [18]. Younger volcanic units are observed mostly in the north and northwest of the accretionary complex. It is reported that the flysch becomes younger from the north to the south of the complex, and its surrounding area becomes shallower from the Cretaceous to the Oligocene, with Oligocene units forming an unconformable cover in the north [19]. The ophiolitic slices within the EAAC represent remnants of the Neotethyan oceanic lithosphere, which was active in the region during the Triassic–Miocene period. These ophiolitic slices are generally represented by isolated, occasionally rodingitized dolerite (diabase) dykes cutting peridotite, gabbro, and peridotite, where the lower parts of the oceanic lithosphere remnants are observed. The effects of accretion and drift can be observed in their structural relationships with the cover rocks (occasionally ophiolite pebbled sandstones with intercalated marl and shale), in the limestone blocks they contain, and in the imbricate systems and folding they exhibit. The units in the study area, from oldest to youngest, are as follows (Figure 2).

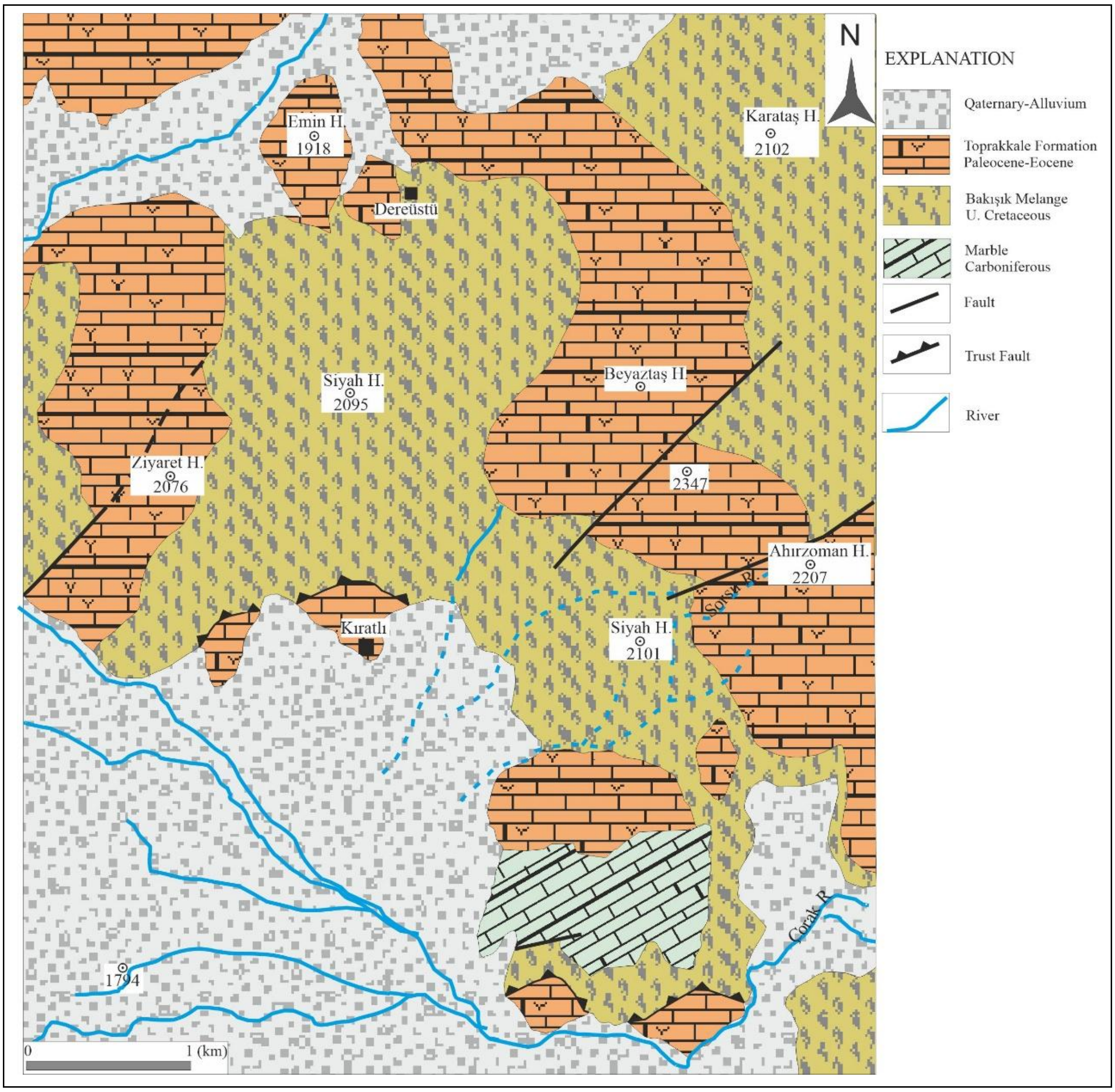

Figure 2. Geological map of the Kıratlı area (İpekyolu–Van) showing the distribution of lithological units, including ultramafic rocks, gabbros, mafic dikes, sedimentary cover units, and alluvial deposits (Modified from [22]).

The oldest unit in the study area is the Carboniferous-aged marble, representing the metamorphic basement rocks. These marbles are tectonically overlaid by the Upper Cretaceous Bakışık Mélange. The Bakışık Mélange, which outcrops extensively in the region, comprises a tectonic mixture of ultramafic–mafic rocks and pelagic sediments. This unit represents the ophiolitic assemblage of the Neo-Tethys Ocean. The Paleocene–Eocene-aged Toprakkale Formation unconformably overlies the Bakışık Mélange. This formation consists primarily of limestone, marl, and calcareous mudstone, reflecting marine carbonate sedimentation in a continental margin environment on a regional scale [20]. The youngest units in the region are Quaternary alluvial deposits, consisting of gravel, sand, and clay-sized materials transported by rivers and deposited in valleys, particularly in the western and southwestern parts of the study area. The lithological units in the area are cut by east–west trending normal and thrust faults, which control the spatial distribution and orientation of the rock units.

The Bakışık Melange, formed at the end of the Late Cretaceous, consists of serpentinite, harzburgite, dunite, gabbro, radiolarite, chert, shale, limestone, and claystone. Because of its very complex structure, it is also referred to as the complex series [21]. It has been stated that the Bakışık Melange was formed by the convergence of numerous rock types of varying ages, in a complex tectonic relationship [22]. The unit, composed of rock types such as serpentinite, harzburgite, dunite, diabase dykes, gabbro, etc., has a rather complex structure. Frequent lateral changes in rock type are observed within the unit, and clastic rocks such as sandstone, conglomerate, and siltstone are also observed here and there [23].

The ultramafic rocks observed in the study area are generally composed of harzburgite and dunite. Carbonate rocks (limestone and marble) lie below these units, while mafic rocks overlie them. Gabbros, observed within the Bakışık Melange in the study area, are occasionally observed as dykes and massive masses (Figure 3a). It is gray-black in color and has fine-to-medium grains (100 μm-2 mm). Crystalline components can be easily identified with the naked eye and a hand lens (Figure 3b). Gabbros, which form outcrops on the topography, exhibit abundant fractures and fissures. Intense serpentinization is noted in the margins of microgabbro dykes that cut through ultramafic rocks of harzburgite composition within the Bakışık Melange (Figure 3c). A mesh texture is commonly observed in the serpentinites formed at the dyke margins.

Isolated Diabase Dykes, observed as hard outcrops with grayish and black hues and sharply demarcated from the host rocks, range in size from five to ten meters. Diabase dykes are found brecciated in areas where tectonism has been active, cutting through serpentinites. They have a massive appearance in the field. Diabase dykes have undergone extensive alteration. In some areas, diabase dykes have acquired characteristics completely different from their original setting. Altered diabase dykes are typically whitish-green in color (Figure 3d). As a result of alteration, diabase dykes turn into rodingites, but their primary properties are preserved in the inner parts of the dykes (Figure 3c).

Figure 3. Field photographs of (a): Mafic and ultramafic units in the study area. (b): Outcrop of massive gabbro within the Bakışık Melange. (c): Rodingitized diabase dike. (d): Mafic dikes cross-cutting ultramafic rocks.

3 Materials and Methods

This study focuses on the mafic rocks exposed within the Bakışık mélange (İpekyolu–Van), covering an area of approximately 15 km^2 around the village of Kıratlı. The main objective is to describe the lithological characteristics, mineralogical–petrographic features, and textural relationships of these mafic rocks in order to elucidate their petrogenesis. Representative rock samples were systematically collected based on field observations, and essential photographic documentation was carried out to support petrographic and geochemical evaluations. A detailed 1:25000 scale geological map of the study area was prepared using the 1:500000 scale regional geological map published by the General Directorate of Mineral Research and Exploration (MTA) as a base reference.

In the laboratory phase, thin sections were prepared from selected mafic rock samples. Petrographic analyses were conducted using transmitted light microscopy to determine the mineralogical composition and textural features of the rocks. For geochemical characterization, 12 representative rock samples were analyzed by ACME Laboratories. Major oxide concentrations were determined using Inductively Coupled Plasma–Emission Spectrometry (ICP-ES) and reported as weight percentages (wt.%), while trace element contents were analyzed using Inductively Coupled Plasma–Mass Spectrometry (ICP-MS) and reported in parts per million (ppm).

4 Results

4.1 Petrography

Mafic rocks are generally observed as dikes intruding the ultramafic units, and field observations indicate that they were affected by low-grade metamorphism. The dikes are mainly represented by microgabbros and diabases. Plagioclase and pyroxene (orthopyroxene+clinopyroxene) are the dominant minerals, and the rocks typically display ophitic texture, with randomly oriented plagioclase laths enclosing anhedral pyroxene crystals (Figure 4a). Alteration is marked by widespread chloritization and, locally, sericitization.

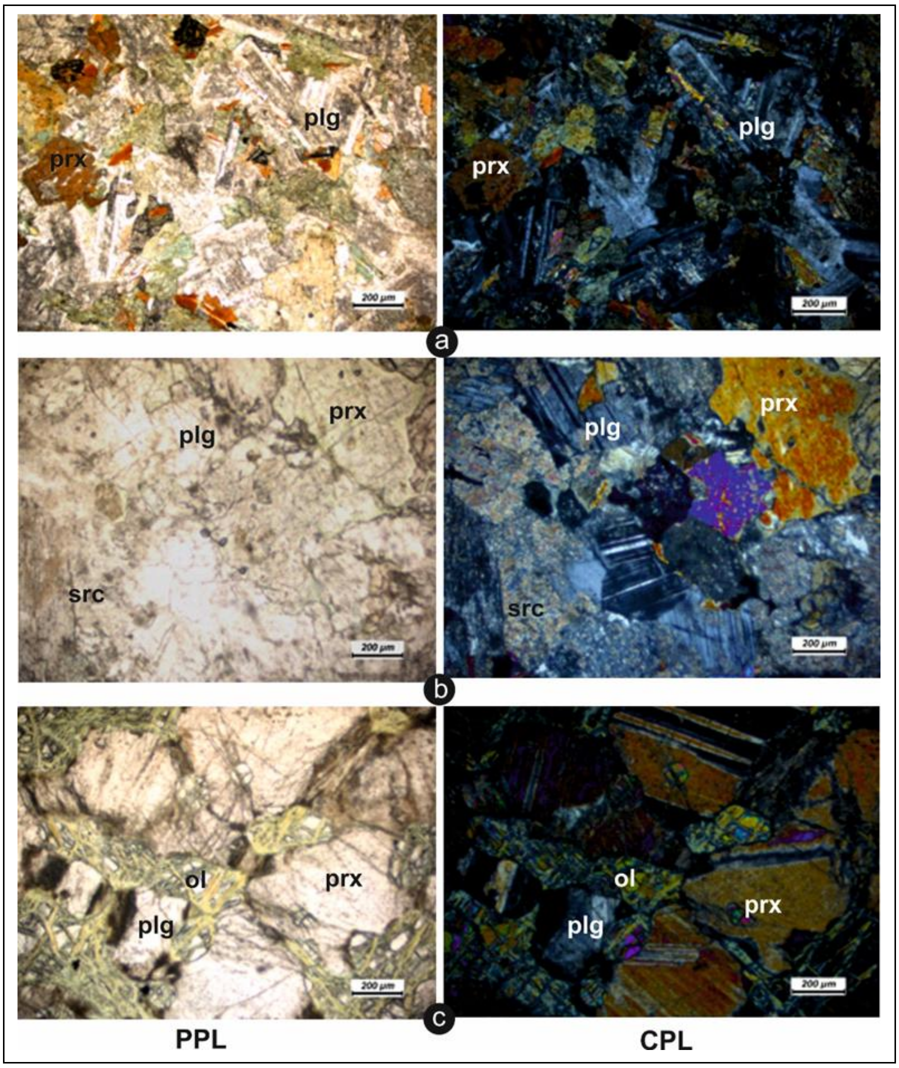

Figure 4. Photomicrographs of mafic rocks from the Kıratlı area. (a): Ophitic texture with plagioclase laths enclosing pyroxene. (b): Sericitization of plagioclase crystals. (c): Pyroxene and fractured olivine grains. PPL: Parallel, CPL: Crossed nicols.

Plagioclase occurs as tabular and prismatic crystals, making up about 60–65% of the rock. These are mostly subhedral to euhedral, colorless under plane-polarized light, with low relief and first-order interference colors under crossed nicols. Polysynthetic twinning is common, and sericitization is widespread (Figure 4b). Pyroxene, comprising about 35–50%, is mostly subhedral to anhedral, colorless in plane-polarized light, with high relief and second-order interference colors. It typically fills the interstitial spaces between plagioclase laths and is locally altered to chlorite (Figure 4c).

Gabbros occur both as massive bodies and as dikes (microgabbros). They generally exhibit a granular texture, with pyroxenes displaying intergrowths and simple twinning. Plagioclase forms about 45–55% of the rock, occurring as subhedral to euhedral crystals with low relief and first-order interference colors, and typically shows polysynthetic twinning (Figure 4b). Sericitization of plagioclase is common. Pyroxene constitutes ~30–40% of the rock, is generally subhedral to anhedral, colorless, with high relief, and shows second-order interference colors (Figure 4b). Olivine is present in minor amounts (2–5%) and is easily recognized by its high relief and vivid interference colors under crossed nicols. It occurs as small, fractured, anhedral to subhedral grains (Figure 4c).

4.2 Geochemistry

Analysis of the major oxide data for the mafic rocks shows SiO_2 values ranging from 42.35–50.95 wt.% and Cr_2O_3 values from 0.01–0.12 wt.% (LOI = 2.4–8.1 wt.%)(Table 1). Trace element concentrations vary significantly, with Ni ranging from 22.4 to 930.1 ppm and Co from 24.2 to 68.2 ppm. Such variability is interpreted to reflect secondary alteration and/or the presence of secondary hydrous or carbonate phases [24]. Due to alteration processes that occurred after rock formation, mobility of major and certain trace elements, particularly large-ion lithophile elements (LILE), can be observed [25-[27]. Therefore, in petrological studies, rare earth elements (REE) and high field strength elements (HFSE), which are resistant to alteration, are preferred [28]-[30]. For this reason, the classification of the mafic rocks in this study was based on the [31] diagram. Overall, the samples are basaltic in composition and can be divided into two groups: alkaline and subalkaline basalts (Figure 5a). The subalkaline samples were further plotted on a SiO_2–FeO/MgO diagram to determine whether they are tholeiitic or calc-alkaline in character. The results show that all subalkaline samples fall within the tholeiitic field (Figure 5b).

The major oxide variation diagrams of the Kıratlı mafic dikes display two distinct evolutionary trends corresponding to the tholeiitic and alkaline basaltic groups (Table 1 and Figure 6). The tholeiitic dikes are characterized by a systematic decrease in MgO and CaO with increasing SiO_2, coupled with a pronounced rise in FeO/MgO ratios, indicating Fe enrichment typical of tholeiitic differentiation trends (Figure 6 and Figure 7a) (FeO = 0.8998 × Fe2O3, from [33]). These relationships suggest that fractional crystallization was dominated by early olivine and clinopyroxene removal, followed by progressive iron enrichment during melt evolution. The relatively constant or slightly decreasing Al_2O_3 values are consistent with limited plagioclase crystallization during early stages.

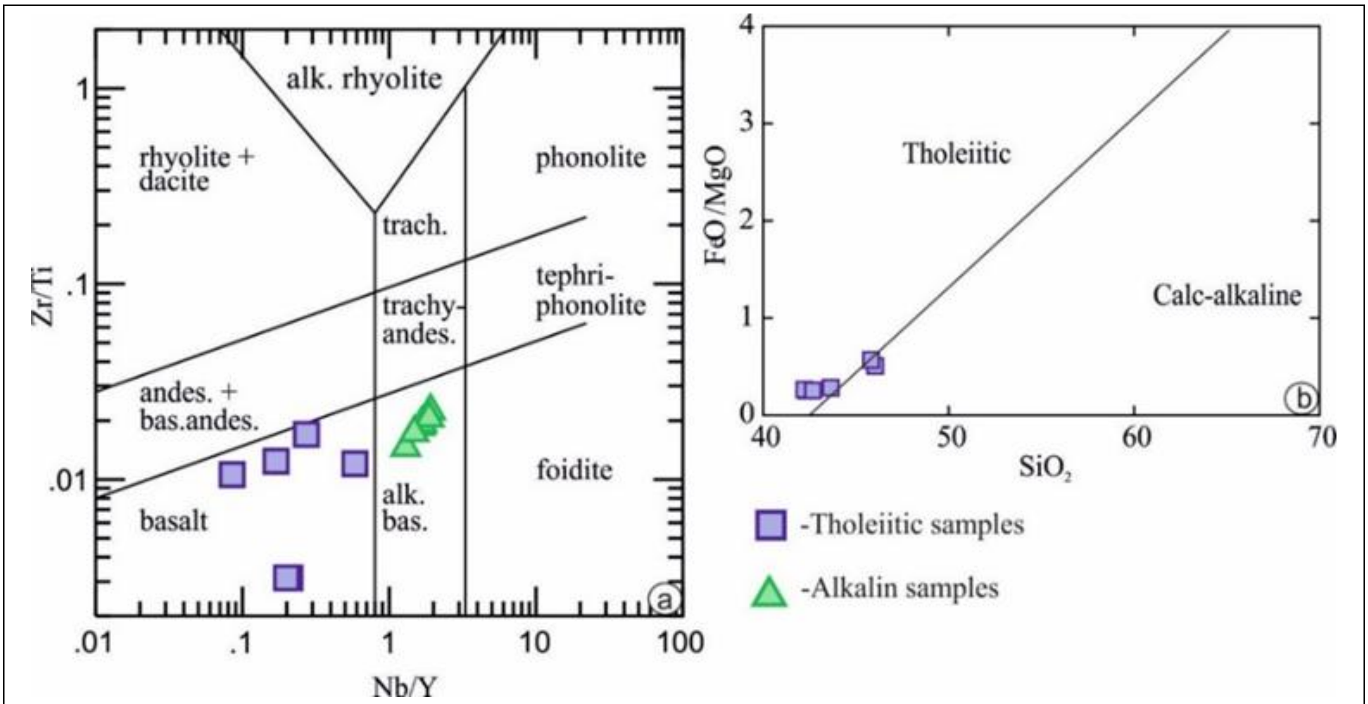

Figure 5. Geochemical classification diagrams. (a): Zr/Ti vs Nb/Y discrimination diagram (after [31]) showing the geochemical classification of the studied volcanic rocks. (b): FeO/MgO vs SiO_2 diagram (after [32]) distinguishing tholeiitic and calc-alkaline affinities.

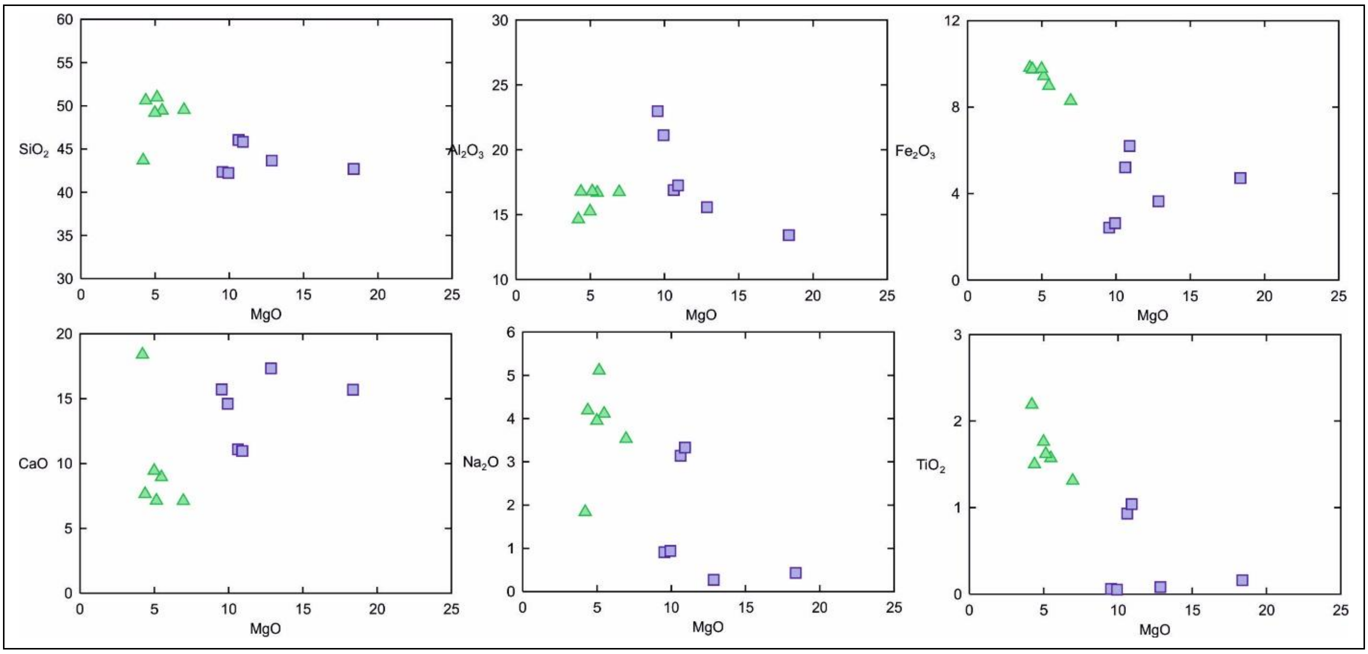

Figure 6. MgO(wt.%) vs. major oxide elements (wt.%) variation diagrams illustrating the effects of fractional crystallization and magma evolution trends for the studied mafic rocks (symbols as in Figure 5).

Table 1. Major oxide (wt.%), Trace element (ppm), and REE (ppm) analyses of mafic dikes.

	DYK-4	DYK-19	DYK-23	LK-16	LK-6	LK-41	LK-38	DYK-8	LK-18	LK-7	DYK-5	DYK-1
SiO_2	42.35	46.04	45.82	42.23	43.65	42.69	49.43	49.52	43.69	50.95	50.6	49.17
Al_2O_3	22.97	16.88	17.25	21.12	15.57	13.421	16.68	16.73	14.65	16.79	16.76	15.25
Fe_2O_3	2.43	5.21	6.2	2.63	3.64	4.72	8.98	8.29	9.82	9.43	9.75	9.77
MgO	9.54	10.63	10.92	9.9447	12.86	18.38	5.48	6.95	4.2	5.14	4.38	4.99
CaO	15.71	11.1	10.974	14.61	17.34	15.69	8.95	7.12	18.4	7.14	7.65	9.44
Na_2O	0.91	3.14	3.33	0.94	0.27	0.43	4.11	3.53	1.84	5.11	4.19	3.95
K_2O	0.7	1.02	0.35	0.27	0.46	0.14	0.98	2.19	0.67	0.59	1.63	1.42
TiO_2	0.06	0.93	1.036	0.05	0.08	0.16	1.57	1.31	2.19	1.62	1.5	1.76
P_2O_5	0.01	0.48	0.31	0.01	0.02	0.03	0.39	0.43	0.42	0.41	0.52	0.35
MnO	0.05	0.32	0.17	0.05	0.07	0.13	0.15	0.16	0.17	0.16	0.15	0.16
LOI	4.8	3.96	3.01	8.1	5.7	3.8	3	3.4	3.7	2.4	2.6	3.5
Total	99.53	99.71	99.37	99.95	99.66	99.59	99.72	99.63	99.75	99.74	99.73	99.76
Cr_2O_3	0.12	0.11	0.14	0.09	0.06	0.21	0.02	0.01	0.00	0.01	0.01	0.01
Ba	208	211	198	25	35	86	191	533	238	100	384	377
Sc	10	30	48	4	41	34	24	20	23	25	21	25
Co	29.5	36	43	40.7	42.2	68.2	29.9	24.2	32.8	30.5	28.8	30.9
Ni	109.6	144	157	930.1	109.6	482.1	34.2	37.2	22.7	27.2	22.4	29.5
Ga	8.4	14	16	6.4	5.9	3.9	13.5	13.8	14	14.3	15	14.1
Hf	0.6	5.2	3.1	0.4	0.2	0.2	3.6	3.7	4.2	3.8	3.7	3.9
Nb	0.3	4	2.1	0.7	0.4	0.9	41.4	49.9	35.8	45.7	52.8	39.2
Rb	9.8	9.6	7.5	3.7	10.3	2.1	15.7	32.1	8.4	10.5	19.2	25.8
Sr	1061.2	402	196	1003.5	267.7	142.4	315.7	362.3	268.7	415.2	461.6	226.2
Ta	1.8	2.2	2.4	2.3	2.1	nd	2.2	2.7	2.3	2.2	3	2.7
Th	2.1	2.42	1.9	1.6	2.3	1.9	4.3	6.1	3	6	6.8	3.8
U	0.6	2.1	3.1	0.6	1	1.8	1.2	1.9	0.6	1.4	2.1	0.9
V	30	216	187	22	82	120	164	162	192	174	193	177
W	nd	nd	nd	nd	nd	0.9	nd	nd	nd	1.4	0.6	0.6
Zr	6.1	6.9	5.9	3.6	1.5	3	174.8	175.6	190.4	187.2	184.6	181.9
Y	1.1	3.6	4.6	1.2	1.9	4.5	25.4	26.1	27.6	27.3	28.1	26.5
La	0.5	1.9	1.3	1.2	0.4	0.3	38.4	49.7	29	45.8	49.8	38.8

Table 1. Continued.

	DYK-4	DYK-19	DYK-23	LK-16	LK-6	LK-41	LK-38	DYK-8	LK-18	LK-7	DYK-5	DYK-1
Ce	1.4	5.8	6.3	1.1	2.5	6.5	72.1	67.7	55.7	82.9	91.62	68.1
Pr	0.08	0.08	0.06	0.1	0.06	0.11	7.81	9.45	6.62	8.91	10.7	7.41
Nd	11.9	13.9	14.3	0.5	0.5	0.7	29.9	34.5	26.9	33.1	39.7	27.6
Sm	0.08	0.28	0.05	0.15	0.13	0.33	5.64	5.8	5.52	6.25	6.65	5.45
Eu	0.19	0.8	0.9	0.1	0.1	0.22	1.8	1.81	1.94	1.9	2.02	1.69
Gd	0.18	0.96	0.06	0.18	0.28	0.069	5.53	5.62	6.08	6.27	6.29	5.63
Tb	0.02	0.05	0.02	0.03	0.05	0.13	0.82	0.86	0.92	0.92	0.96	0.85
Dy	0.32	0.16	0.09	0.21	0.32	0.88	5.02	4.65	5.33	5.43	5.18	4.78
Ho	0.06	0.05	0.08	0.04	0.09	0.17	0.98	0.97	1.08	1.1	1.08	0.99
Er	0.21	0.16	0.12	0.11	0.21	0.59	2.55	2.89	3.14	3.08	2.94	2.75
Tm	0.02	0.09	0.03	0.01	0.02	0.08	0.37	0.38	0.42	0.43	0.43	0.39
Yb	0.15	0.18	0.26	0.18	0.15	0.47	2.38	2.49	2.65	2.65	2.75	2.42
Lu	0.02	0.02	0.02	0.02	0.02	0.06	0.37	0.37	0.38	0.44	0.41	0.36
TOT/C	0.05	0.03	0.2	0.05	0.05	0.03	0.03	0.05	0.05	0.02	0.02	0.06
Mo	1	0.8	0.6	1	1	0.5	0.5	1.3	1.4	0.4	0.7	3
Cu	122.4	78.6	86.2	464.3	178	77	68.1	70.6	60.1	142.9	55.9	77
Pb	0.3	0.3	0.4	0.8	0.3	1.5	2.3	2.7	2.5	2.5	1.8	1.4
Zn	7	27	32	6	7	23	34	26	45	42	28	52

In contrast, the alkaline dikes exhibit higher total alkali (Na_2O + K_2O) contents and elevated FeO/MgO ratios at comparable MgO levels, implying derivation from a more enriched mantle source (Figure 7b, c). Their Al_2O_3 contents show a broader range, possibly reflecting variable plagioclase fractionation and accumulation. CaO values remain relatively high compared to the tholeiitic series, supporting a distinct magmatic evolution pathway rather than a single fractional crystallization trend. These features, together with the incompatible element variations (e.g., Zr, Yb, La, Ce), indicate that the alkaline and tholeiitic basalts originated from different mantle sources and followed separate differentiation trajectories, rather than evolving from a common parental magma. Trace element–MgO variation diagrams provide further constraints on magmatic processes (Figure 8). Incompatible elements (e.g., Rb, Ba, Th, Zr, Nb, Y) increase with decreasing MgO, reflecting their progressive enrichment in residual melts during fractional crystallization. Conversely, compatible elements such as Ni, Co, and Sc decrease with decreasing MgO, consistent with early crystallization and removal of olivine and pyroxene. These systematic trends indicate that the primitive melts were mantle-derived, evolving through fractional crystallization of mafic phases. The relatively high Th contents and negative Nb anomalies point to subduction-derived fluids enriching the mantle source [34],[35]. Thus, the geochemical trends observed in Figure 8 support a supra-subduction zone affinity with evidence of mantle heterogeneity. To determine the tectonic setting of mafic rocks, stable trace elements (Ti, V, Zr, Y, and Nb), which are less affected by alteration and low-grade metamorphism, are widely employed. Numerous discrimination diagrams have been proposed to constrain the tectonomagmatic setting of igneous rocks, most of which rely on trace element contents of volcanic rocks.

The Nb/Yb and Th/Yb ratios can distinguish between depleted and enriched mantle sources [35]. In subduction zones, slab-derived melts and fluids enrich the mantle wedge, resulting in elevated Th/Yb ratios.

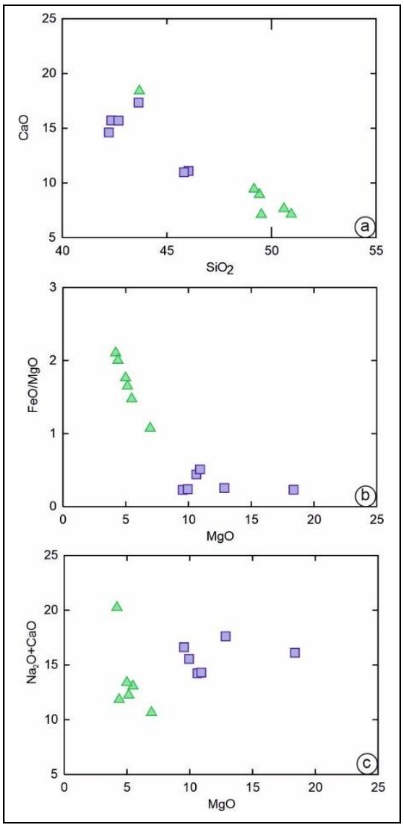

Figure 7. Major element variation diagrams for the Kıratlı mafic dikes. (a): CaO vs. SiO_2, (b): FeO/MgO vs. MgO, and (c): (Na_2O + K_2O) vs. MgO. The negative correlations between MgO and FeO/MgO and between MgO and CaO indicate progressive fractional crystallization dominated by early olivine, clinopyroxene, and plagioclase removal. Higher total alkali contents and FeO/MgO ratios in the alkaline dikes relative to the tholeiitic dikes, suggest derivation from a more enriched mantle source.

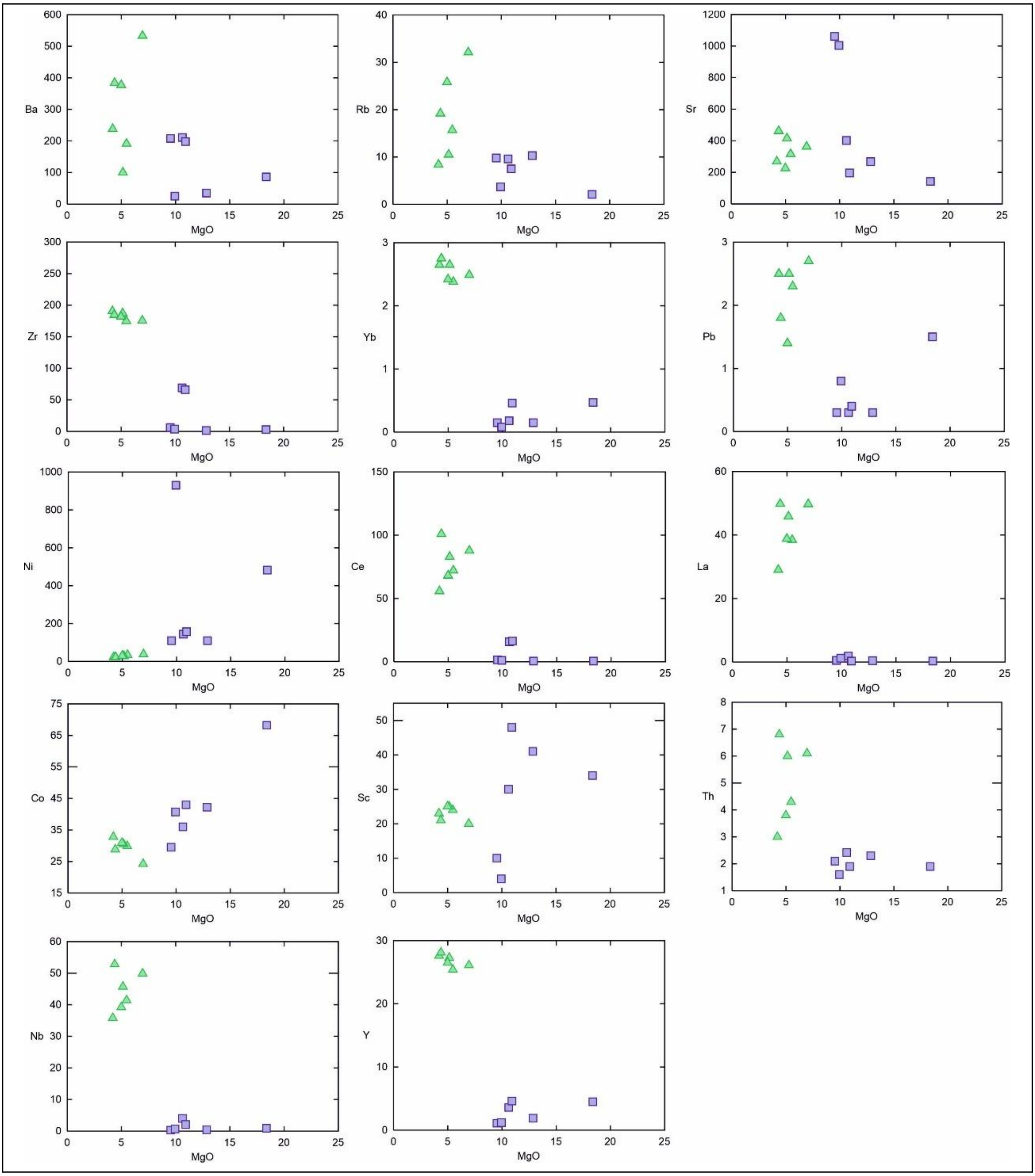

Figure 8. Variation diagrams showing the relationships between MgO and selected trace elements (Ba, Rb, Sr, Zr, Yb, Pb, Ni, Ce, and La) for the studied diabase and microgabbro samples. The plots illustrate systematic decreases in compatible elements such as Ni and Sr with decreasing MgO, reflecting fractional crystallization of mafic minerals. Incompatible elements (e.g., Ba, Rb, Zr, Ce, and La) generally increase as MgO decreases, indicating progressive magma differentiation. (Symbols as in Figure 5).

According to this diagram, the tholeiitic mafic rocks associated with the ophiolite sequence were derived from a depleted mantle source and formed in a supra-subduction zone environment, whereas the alkaline mafic rocks are indicative of an oceanic island arc setting. The overall data, based on [35] Nb/Yb–Th/Yb diagram, suggest that the studied units correspond to mid-ocean ridge and island arc ophiolites (Figure 9a).

Further constraints on the magmatic setting were obtained using Th-Zr/117-Nb/16 ternary diagram [36]. The alkaline samples plot within the within-plate alkali basalt field, whereas the tholeiitic samples fall within the island arc basalt field (Figure 9b).

On the V–Ti discrimination diagram of [37], some samples fall into the island arc tholeiite (IAT) field, while four samples plot within the mid-ocean ridge basalt (MORB) field, suggesting transitional affinities between arc-related and MORB-type basalts (Figure 9c). Chondrite-normalized rare earth element (REE) patterns of the mafic rocks are presented in Figure 10a. The alkaline basalts exhibit moderately LREE-enriched patterns, with $(La/Yb)_N$ =7.43-13.55, indicating enrichment similar to those of oceanic arc basalt types. In contrast, the tholeiitic basalts display depleted REE patterns, with $(La/Yb)_N$ values between 0.43 and 7.17 reflecting partial melting of a depleted mantle source N-MORB–normalized spider diagrams reveal enrichment in large-ion lithophile elements (LILE; e.g., Sr, Rb, K, Ba, Th) and depletion in high field strength elements (HFSE), while maintaining parallel trends to the normalized MORB line (Figure 10b). LILE enrichment reflects the transfer of fluid-mobile components from the subducting slab to the overlying mantle wedge, whereas elements that parallel the tholeiitic trend indicate a mantle-derived component. The most striking features of the diagram are the positive Th anomaly and the negative Nb anomaly, both diagnostic of subduction-related signatures [39].

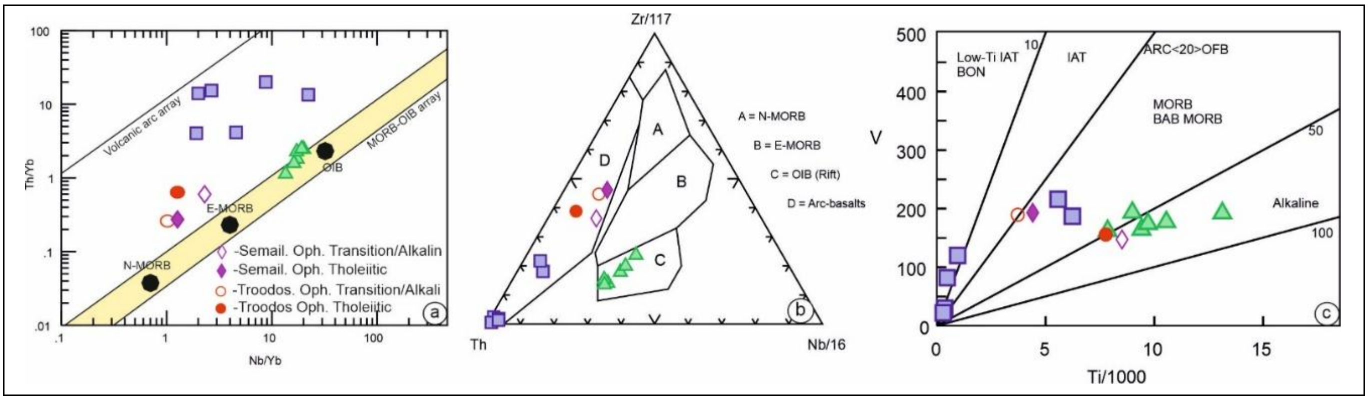

Figure 9. Tectonomagmatic discrimination diagrams. (a): Nb/Yb–Th/Yb plot showing depleted mantle sources for tholeiitic dikes and enriched signatures for alkaline dikes after [35]. (b): Th–Zr–Nb ternary diagram distinguishing within-plate alkali basalts and island-arc basalts after [36]. (c): V–Ti diagram with samples plotting in IAT and MORB fields after [37]. BAB = backarc basin; EMORB = enriched mid-ocean ridge basalt; NMORB = normal mid-ocean ridge basalt; OIB = ocean-island basalt; (Comparison data for the Troodos and Semail ophiolites are derived from [38]and [39], symbols as in Figure 5).

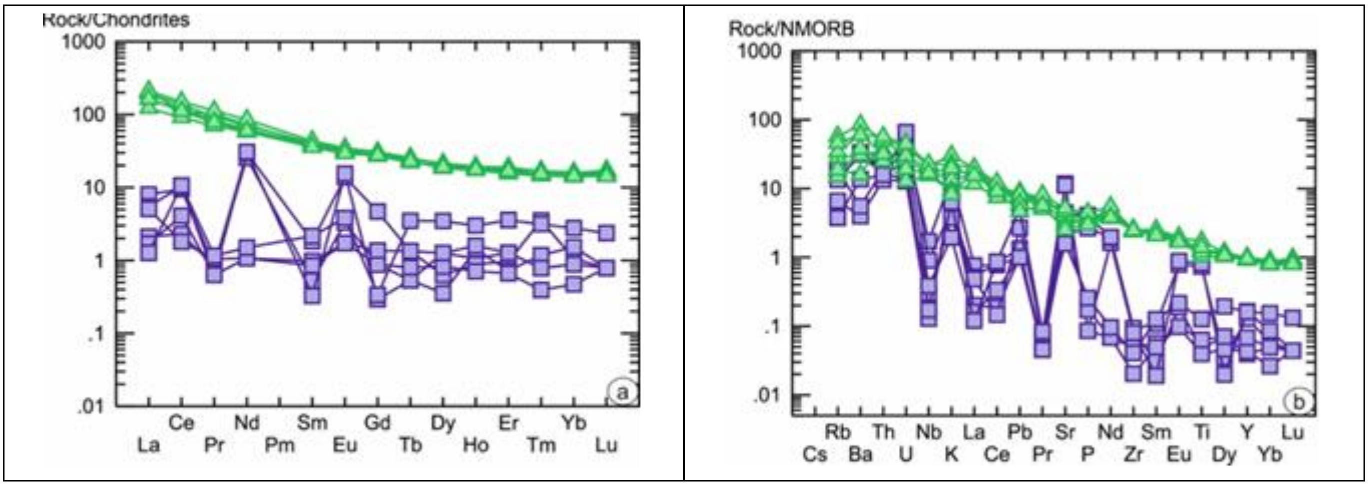

Figure 10. Normalized geochemical patterns of the Kıratlı mafic rocks. (a) Chondrite-normalized. (b) N-MORB–normalized multi-element spider diagram (Chondrite and N MORB Normalized values of [42]; symbols as in Figure 5).

5 Discussion

Isolated mafic dikes are widespread features in ophiolitic complexes, intruding ultramafic rocks such as harzburgite and lherzolite. Unlike sheeted dike complexes, these intrusions occur as scattered or irregular bodies, reflecting localized magma supply and tectonic control during the evolution of the oceanic lithosphere [3], [41]. In the Kıratlı area, the dikes preserve evidence of magmatism associated with both mid-ocean ridge (MORB) and supra-subduction zone (SSZ) settings.

Geochemical data support a dual origin for the studied samples. Tholeiitic samples exhibit LREE enrichment and relatively flat MREE-HREE patterns. This observation suggests that the mantle source was influenced by subduction processes; in contrast, alkaline samples exhibit LREE-enriched signatures and intraplate affinities. These patterns suggest low-degree partial melting or crustal contributions during extensional stages, a feature reflecting the multiphase magmatism common in ophiolitic sequences [4].

Major oxides plotted against MgO exhibit clear trends of decreasing CaO and increasing Fe_2O_3 and TiO_2 with decreasing MgO, indicative of fractional crystallization. These geochemical variations suggest progressive removal of olivine, pyroxene, and plagioclase, leading to magma evolution toward more Fe–Ti–alkali-enriched compositions. The data strongly support fractional crystallization as the dominant differentiation process in the Kıratlı mafic dikes (Figure 6). The chondrite-normalized REE patterns of the Kıratlı mafic dikes reveal distinct behaviors for the tholeiitic and alkaline series (Table 1 and Figure 8). The tholeiitic dikes exhibit slightly depleted LREEs and a modest positive Eu anomaly, whereas the alkaline dikes display nearly flat REE patterns without significant Eu anomalies. The positive Eu anomaly in tholeiitic samples may reflect plagioclase accumulation within the magma chamber, rather than simple fractionation, consistent with fractional crystallization trends inferred from major oxides (e.g., decreasing MgO and CaO). Alternatively, the anomaly could indicate a source-related signature, suggesting that the tholeiitic magmas derived from a slightly plagioclase-rich mantle source or experienced minor crustal assimilation. The absence of Eu anomalies in alkaline dikes implies limited plagioclase involvement, consistent with their more enriched, high-alkali nature. Overall, the REE data indicate that Eu anomalies are controlled by a combination of magmatic differentiation processes and source characteristics, differing between the tholeiitic and alkaline series. These features are comparable to dike suites in the Troodos and Semail ophiolites, where multistage magmatic processes have also been documented [38],[39]. Regional comparisons further highlight the significance of the Kıratlı dikes. Their transitional to tholeiitic affinities are similar to those reported from the Pozantı–Karsantı, Kızıldağ, and Guleman ophiolites [43], [44]. They also resemble mafic intrusions from the İzmir–Ankara–Erzincan Suture Zone, indicating that polyphase magmatism affected both the northern and southern branches of the Neo-Tethys. This suggests that heterogeneous mantle sources, subduction-related enrichment, and extensional tectonics collectively shaped the magmatic evolution across the entire Neo-Tethyan domain.

Taken together, the Kıratlı dikes represent a record of multi-stage magmatism within an evolving back-arc basin, overprinted by later extensional processes. Their geochemical variability underscores the complex interplay of mantle melting, subduction modification, fractional crystallization, and tectonic extension in the southeastern Anatolian ophiolite belt.

6 Conclusion

Petrographic and geochemical analyses of the Kıratlı mafic dikes reveal a polygenetic magmatic history linked to the closure of the Neo-Tethys. The coexistence of tholeiitic and alkaline compositions reflects melts derived from heterogeneous mantle sources that experienced varying degrees of partial melting, fractional crystallization, and crustal interaction.

Trace element systematics, including LILE enrichment, Nb depletion, and variable REE patterns, point to a supra-subduction zone affinity for the tholeiitic dikes, whereas the alkaline dikes indicate later extensional magmatism. These results are consistent with similar dike suites documented in other ophiolites of Türkiye and demonstrate that polyphase magmatism was not restricted to a single branch of the Neo-Tethys but instead influenced both northern and southern branches.

Overall, the Kıratlı dikes provide new insights into the complex tectono-magmatic evolution of the southeastern Anatolian Ophiolite Belt. They record evidence of back-arc basin magmatism overprinted by extensional processes, highlighting the dynamic nature of mantle melting and magma emplacement during the progressive closure of the Neo-Tethys.

7 Acknowledgment

This study was supported by the Scientific Research Projects Directorate of the Van Yüzüncü Yıl University under the project number 2015-FBE-YL 252. This work forms part of Hakan Yazıcıoğlu's master's thesis.

8 Author contribution statements

Fieldwork and petrographic analyses were supported by Hakan Yazıcıoğlu. Tijen Üner contributed to the fieldwork, petrographic analyses, and geochemical investigations. The manuscript was prepared and written by Tijen Üner. Ethics committee approval and conflict-of-interest statement.

9 Ethics committee approval and conflict of interest statement

"Ethics committee permission is not required for the article prepared". "There is no conflict of interest with any person/institution in the article prepared".

10 References

[1] Şengör AMC, Yılmaz Y. "Tethyan Evolution of Turkey: A Plate Tectonic Approach". *Tectonophysics*, 75, 181-241, 1981.

[2] Robertson AHF, Karamata S, Saric K. "Overview of ophiolites and related units in the Late Palaeozoic–Early Cenozoic magmatic and tectonic development of Tethys in the northern part of the Balkan region". *Lithos*, 108(1-4), 1-36, 2004.

[3] Pearce JA. *Trace Element Characteristics of Lavas from Destructive Plate Boundaries*. Editor: Thorpe RS, Andesites: Orogenic Andesites and Related Rocks, 252-548, Chichester, England: John Wiley and Sons, 1982.

[4] Dilek Y, Furnes H. "Ophiolite genesis and global tectonics: Geochemical and tectonic fingerprinting of ancient oceanic lithosphere". *Geological Society of America Bulletin*, 123, 387–411, 2011.

[5] Pearce, JA. *Geochemical Evolution for the Genesis and Eruptive Setting of Lavas from Tethyan Ophiolites*. Editor: Panayiotou A. *Opiolites,* 261-272, Geological Survey Department, Cyprus, 1980.

[6] Hawkins JW, Bloomer SH, Evans CA, Melchior JT. "Evolution of intra–oceanic arc–trench systems". *Tectonophysics*, 102, 175–205, 1984.

[7] Parlak O, Höck V, Delaloye M. "Suprasubduction zone origin of the Pozanti-Karsanti ophiolite (Southern Turkey) deduced from whole-rock and mineral chemistry of the gabbroic cumulates". *Geological Society, London, Special Publications*, 173(1), 219-234, 2000.

[8] Dilek Y, Thy P. "Island arc tholeiite to boninitic melt evolution of the Cretaceous Kizildag (Turkey) ophiolite: Model for multi-stage early arc-forearc magmatism in Tethyan subduction factories". *Lithos*, 113, 68–87, 2009.

[9] Çimen O, Önal, AÖ. "Preliminary geochemical data of the mafic rocks from the Ovacik and Pülümür Ophiolite Zone (Eastern Anatolia, Turkey): implications for the geodynamic evolution of the Northern Neotethyan Ocean". *Ofioliti*, 43(2), 103-116, 2018.

[10] Bağcı U, Parlak O, Höck V. "Geochemical character and tectonic environment of ultramafic to mafic cumulate rocks from the Tekirova (Antalya) ophiolite (southern Turkey)". *Geologıcal Journal*, 41, 193-219, 2006.

[11] Elitok Ö, Dolmaz MN. *Tectonic Escape Mechanism in the Crustal Evolution of Eastern Anatolian Region (Turkey)*. Editor: Schattner, U. *New Frontiers in Tectonic Research-At the Midst of Plate Convergence*, 289-302, Open Access Peer-Reviewed Edited Volume, 2011.

[12] Yılmaz Y. "New evidence and model on the evolution of the southeast anatolian orogen". *Geological Society of American Bulletin*, 105, 251-271, 1993.

[13] Bozkurt E. "Neotectonics of Turkey-a Synthesis". *Geodinamica Acta*, 13(1-3), 3-30, 2001.

[14] Koçyiğit A, Yılmaz A, Adamia A, Kuloshvili S. "Neotectonics of East Anatolian Plateau (Turkey) and Lesser Caucasus: Implication for Transition From Thrusting To Strike-Slip Faulting". *Geodinamica Acta*, 14, 177–195, 2001.

[15] Barazangi M, Sandvol E, Seber D. "Structure and tectonic evolution of the Anatolian plateau in eastern Turkey". *Geological Society of America Special Paper*, 409, 463-473, 2006.

[16] Şengör AMC, Özeren MS, Keskin M, Sakınç M, Özbakır AD, Kayan İ. "Eastern Turkish high plateau as a small Turkic-type orogen: Implications for post-collisional crust-forming processes in Turkic-type orogens". *Earth- Science Reviews*, 90, 1–48, 2008.

[17] Göncüoğlu MC, Dirik K, Kozlu H. "General chracteristics of pre-Alpine and Alpine Terranes in Turkey: Explanatory notes to the terrane map of Turkey". *Annales Geologique de Pays Hellenique*, 37, 515-536, 1997.

[18] Okay AI, Tüysüz O. "Tethyan sutures of northern Turkey". *Geological Society, London, Special Publications*, 156, 475–515, 1999.

[19] Tüysüz N, Erler A. "Geology and geotectonic implications of Kazıkkaya area, Kağızman-Kars (Turkey)". *Proceedings of the International symposium on the Geology of the Black sea Region*, Ankara, Turkey, 7-11 September 1995.

[20] Şengör AMC, Özeren S, Genç T, Zor E. "East Anatolian high plateau as a mantle-supported, north-south shortened domal structure". *Geophysical Research Letters*, 30(4), 8045, 2003.

[21] Saydamer M. "İran Sınırı Boyunca Yapılan Jeolojik Çalışmanın Nihai Raporu". MTA Genel Müdürlüğü, 5622, Ankara, 1976.

[22] Acarlar M, Bilgin A, Erkal T, Güner E, Şen A, Umut M, Elibol E, Gedik İ, Hakyemez Y, Uğuz F. "Van Gölü ve Kuzeyinin Jeolojisi". Van, MTA Raporu, 9469, 1991.

[23] Ateş S, Mutlu G, Özerk OC, Çiçek İ, Karakaya Gülmez F, Bulut Ü A, Karabıyıkoğlu M, Osmançelebioğlu R, Özata A, Aksoy A. "Van İlinin yerbilim verileri". Maden Tetkik ve Arama Genel Müdürlüğü, Ankara, Türkiye, 10961, 2007.

[24] Rollinson HR. *Using Geochemical Data: Evolution, Presentation, Interpretation*. Longman Scientific and Technical, England, 1993.

[25] Hart SR, Erlant AJ, Kable EJD. "Sea floor basalt alteration: some chemical and Sr isotopic effects". *Contributions to Mineralogy and Petrology*, 44, 219-230, 1974.

[26] Humphris SE, Thompson G. "Trace element mobility during hydrothermal alteration of oceanic basalts". *Geochimica et Cosmochimica Acta*, 42, 127–136, 1978.

[27] Thompson TB. Genesis of gold associated with alkaline igneous rocks. *Geological Society of America*, Abstracts with Programs, 23, 99- 100, 1991.

[28] Pearce JA, Cann JR. "Tectonic setting of basic volcanic rocks investigated using trace element analyses". *Earth and Planetary Science Letters,* 19, 290-300, 1973.

[29] Smith RE, Smıth SE. "Comments on the use of Ti, Zr, Y, Sr, K, P and Nb in classification of basaltic magmas". *Earth and Planetary Science Letters*, 32, 114-120, 1976.

[30] Floyd PA, Wınchester JA. "Magma type and tectonic setting discrimination using immobile elements". *Earth and Planetary Science Letters*, 27, 211-218, 1978.

[31] Pearce JA. *User's Guide to Basaltic Discrimination Diagrams*. Editor: Wyman DA. *Trace Element Geochemistry of Volcanic Rocks: Applications for Massive Sulphide Exploration* V.12, 79-113. Geological Association of Canada, Short Course Notes, 1996.

[32] Miyashiro A. "Volcanic rock series in island arcs and active continental margins". *American Journal of Science,* 274, 321–343, 1974.

[33] Le Maitre R W. *Igneous rocks a Classification and Glossary of Terms Recommendations of the International Union of Geological Sciences, Sub-Commission on the Systematics of Igneous Rocks*. 2nd ed. UK, Cambridge University Press, 2002.

[34] Hawkesworth CJ, Gallagher K, Hergt JM, McDermott F. "Mantle and slab contributions in arc magmas". *Annual Review of Earth and Planetary Sciences*, 21, 175–204, 1993.

[35] Pearce JA. "Geochemical fingerprinting of oceanic basalts with applications to ophiolite classification and the search for Archean oceanic crust". *Lithos*, 100, 14-48, 2008.

[36] Wood DA. "The application of a Th-Hf-Ta diagram to problems of tectonomagmatic classification and to establishing the nature of crustal contamination of basaltic lavas of the British Tertiary volcanic province". *Earth and Planetary Science Letters*, 50, 11-30, 1980.

[37] Shervais JW. "Ti-V plots and the petrogenesis of modern and ophiolitic lavas". *Earth and Planetary Science Letters*, 59, 101-118, 1982.

[38] Alabaster T, Pearce JA, Malpas J. "The Volcanic Stratigraphy and Petrogenesis of the Oman Ophiolite Complex". *Contributions to Mineralogy and Petrology*, 81(3), 168–183, 1982.

[39] Pearce J A, Robinson PT. "The Troodos Ophiolite, Cyprus: Magmatic Evolution and Tectonic Setting". *Lithos*, 114(1–2), 1–16, 2010.

[40] Schilling J-G, Zajac M, Evans R, Johnston T, White W, Devine JD, Kingsley R. "Petrologic and geochemical variations along the mid-Atlantic Ridge from 29ON to 73ON". *American Journal of Science,* 283, 510-586, 1983.

[41] Coleman RG. *Ophiolites*. 1st ed. Berlin, Springer-Verlag, 1977.

[42] Sun SS, McDonough WF. "Chemical and isotopic systematics of oceanic basalts: implications for mantle composition and processes". *Geological Society of London Special Publications*, 42, 313–345, 1989.

[43] Nicolas A. *Structure of Ophiolites and Dynamics of Oceanic Lithosphere.* 7th ed. Holland, Kluwer Academic Publishers, 2012.

[44] Parlak O, Höck V, Delaloye M. "The supra-subduction zone Pozanti–Karsanti ophiolite, southern Turkey: Evidence for high-pressure crystal fractionation of ultramafic cumulates". *Lithos*, 65(1–2), 205-224, 2002.